References

1. Mikami, K.; Fugjimoto, K.; Nakai, T. *Tetrahedron Lett.* **1983**, *24*, 513.
2. (a) Mikami, K.; Nakai, T. *Synthesis* **1991**, 594. (b) Marshall, J. A. *Comprehensive Organic Synthesis*, Vol. 3. Trost, B. M.; Fleming, I. (eds).; Pergamon, 1991. (c) Nakai, T.; Mikami, K. *Chem. Rev.* **1986**, *86*, 885.
3. Mikami, K.; Kimura, Y.; Kishi, N.; Nakai, T. *J. Org. Chem.* **1983**, *48*, 297.
4. Mikami, K.; Azuma, K.; Nakai, T. *Tetrahedron* **1984**, *40*, 2303.
5. (a) Marshall, J. A.; Lebreton, J. *J. Org. Chem.* **1988**, *53*, 4108. (b) Marshall, J. A.; Lebreton, J. *J. Org. Chem.* **1992**, *57*, 2747.
6. Hayakawa, K.; Hayashida, A.; Kanematsu, K. *J. Chem. Commun.* **1988**, 1108.
7. Heathcock, C. H.; Buse, C. T.; Kleshick, W. A.; Pirrung, M. C.; Sohn, J. E.; Lampe, J. *J. Org. Chem.* **1980**, *45*, 1066.
8. Ohtani, I.; Kusumi, T.; Kashman, Y.; Kakisawa, H. *J. Am. Chem. Soc.* **1991**, *113*, 4092.
9. Marshall, J. A.; Lebreton, J. *J. Am. Chem. Soc.* **1988**, *110*, 2925.
10. Leinard, N. J.; Thomas, P. D.; Gash, V. W. *J. Am. Chem. Soc.* **1955**, *77*, 1552.
11. Leonard, N. J.; Beyler, R. E. *J. Am. Chem. Soc.* **1950**, *72*, 1316.
12. Neises, B.; Steglich, W. *Organic Synthesis* **1984**, *63*, 183.
13. Dale, J. A.; Dull, D. L.; Mosher, H. A. *J. Org. Chem.* **1969**, *34*, 2543.

Real Time Spectroelectrochemical Experiments with a Multichannel Detector

Sun-il Mho,[1,*] Sally N. Hoier,[2] Bum-Soo Kim, and Su-Moon Park*

Department of Chemistry, University of New Mexico, Albuquerque, NM 87131, U. S. A.
Received March 24, 1994

A spectroelectrochemical system assembled with a white light source, bifurcated optical fiber, Oriel Multispec® spectrograph, and a charge-coupled device (CCD) detector is described. The system is shown to be capable of acquiring a whole spectrum in the spectral range of 290-800 nm in 25 ms or a longer period during electrochemical experiments at reflective working electrodes such as platinum or mercury. The utility of the system in studying electrochemical reactions during the potential scan, galvanostatic electrolysis, or after the potential step is demonstrated.

Introduction

The *in-situ* spectroelectrochemical technique has been used extensively to probe intermediate species during electrochemical studies of electron transfer reactions since its inception by Kuwana *et al.*[1-6] Although the technique has been developed for a variety of electrochemical cells, the most widely used mode of operation is the transmittance measurement at optically transparent electrodes made of conductive metal oxides such as indium-tin oxide (ITO) glass or metal minigrids inside a spectrophotometric cell cuvette. In many of these experiments, the electrochemistry itself presents a limit for fast spectroelectrochemical measurements primarily due to the distorted current path resulting from unfavorable cell geometry among many other parameters. Efforts have been made to improve electrochemical response times by using reflective platinum disk working electrodes and the reflected light beam is measured at glancing angles.[7] Absorbance signals have been measured by this method in microsecond time domains[8]; however, the measurements were made at a single wavelength, which lacks the spectroscopic information. Modification of this method led to a cell, in which a bifurcated optical fiber is located above the reflective working electrode such that the probing and reflected beams would be nearly normal to the working electrode.[9-11] While this geometry allows a spectrum to be measured in a shorter time period, the mechanically driven monochromator now presents a limit to how fast a spectroscopic measurement can be made.

Semiconductor array detectors have been used for spectroscopic measurements for the last decade or so by recording spectrally dispersed light from monochromators.[12] Compared to traditional detectors such as photomultiplier tubes (PMTs), photodiode arrays can acquire data in a multiplexed mode. Of two types of array detectors, *i.e.*, photodiode and charge-coupled device (CCD), the latter has a number of superior features to the former as well as other photon detectors.[13,14] The CCD detectors have a simple dynamic range approaching 1×10^6, spectral response range of about 200-1000 nm, and quantum efficiency of 35-90%. Also, spectral measurements can be made in a microsecond or slower time domain for the whole spectral range by operating in the spectral framing mode. Because of the wide dynamic range of its

[1]On leave from Ajou University, Suwon Korea
[2]Sandia National Laboratories, Albuquerque, NM 87185, U. S. A.

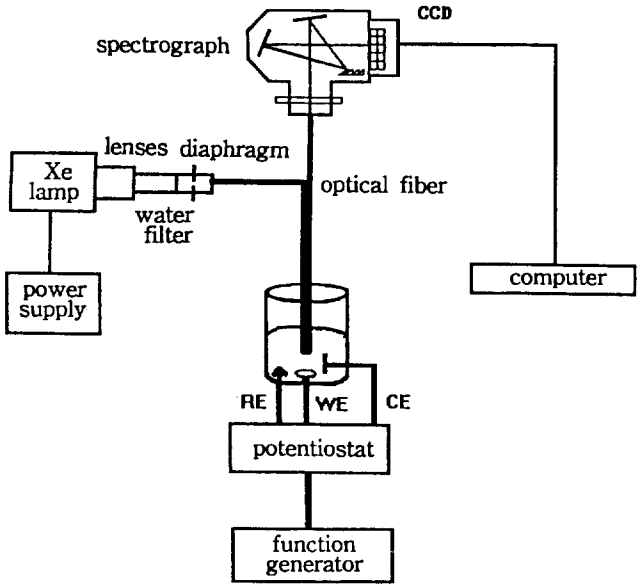

Figure 1. Schematic diagram for the spectroelectrochemical system with a CCD detector.

response, measurements of up to 5 absorbance units are also possible. The CCD-based spectrophotometers have been shown to give high signal-to-noise ratios for spectral measurements of weak signals.[13,14] The technique has been applied to Raman studies at the electrode surfaces.[15-17]

In the present communication, we describe a spectrophotometric system with a CCD detector which allows spectroelectrochemical measurement to be made in faster time domains. Spectra in the whole spectral region were recorded as a function of time after a potential step or as a function of potential during the potential scans.

Experimental

Fischer's reagent grade p-aminophenol (PAP) and Aldrich's methyl viologen (MV) were used after recrystallization. Doubly distilled deionized water was used to prepare the solutions. Experiments were carried out in a 0.10 *M* sulfuric acid with millimolar quantities of these compounds. Thin layer spectroelectrochemical cells were assembled as described earlier.[10] The single compartment cell housed a mercury pool or platinum working electrode, a platinum wire counter electrode, and an Ag/AgCl (in saturated KCl) reference electrode. Electrochemical experiments were conducted with an EG & G Princeton Applied Research (PAR) model 173 potentiostat-galvanostat and a PAR 175 universal programmer.

The spectroelectrochemical system is shown in Figure 1 as a block diagram. As can be seen in this figure, the spectroelectrochemical system is very similar to the one previously described elsewhere.[9-11] The cell geometry is also almost exactly the same as that described earlier. The only difference is the lack of a monochromator between the light source and the entrance branch of the bifurcated optical fiber in the current system. Instead, the white light beam from the source is directed onto the electrode surface through an entrance branch of the optical fiber and an Oriel Multispec® spectrograph with a CCD array detector is attached to the end of the exit branch of the fiber bundle. The CCD output is interfaced to a 386 computer through Oriel's interface board. The light source is a xenon arc lamp. For data acquisition, a canned program provided by Oriel was used.

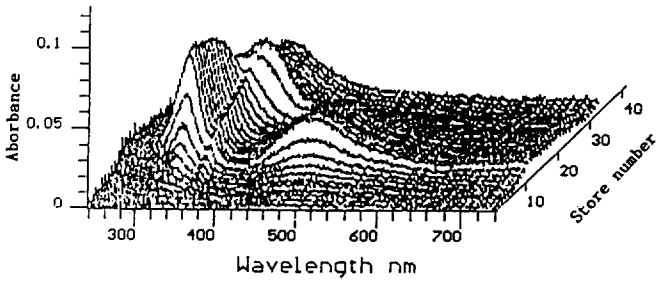

Figure 2. Spectra recorded from 19.0 mM MV^{2+} in 3.0 M KCl during electrolysis at -60 μA at a Hg pool electrode. Each spectrum was obtained by 20 ensemble averaging for 0.5 s.

Results and Discussion

Two electrochemical systems were used for the evaluation of the system. The first is the reduction of methyl viologen (MV^{2+}) in two steps according to:

$$MV^{2+} + e^- \rightarrow MV^+ \quad (1)$$

and

$$MV^+ + e^- \rightarrow MV^0 \quad (2)$$

As the neutral species undergoes a fast reproportionation reaction with MV^{2+} ($k_f = 6.3 \times 10^7\ M^{-1}$)

$$MV^0 + MV^{2+} \rightarrow 2MV^+ \quad (3)$$

efficiently, an exhaustive electrolysis cell must be used for recording spectra of electrogenerated species, MV^+ and MV^0. For this reason, we used a thin layer cell (TLC).

Figure 2 shows a series of spectra recorded during galvanostatic electrolysis of a 19.0 mM MV^{2+} solution in a TLC with a reflective mercury pool working electrode. It is seen clearly in the figure that reactions (1) and (2) occur sequentially as the electrolysis proceeds. The cation radical (MV^+) is seen to increase at the initial stage of the electrolysis, which begins to recede at longer times than 10 s (store number 20) as evidenced by the growth and fall of the band at around 490 nm. This band was assigned to the dimer of the methyl viologen radical cation.[11,18,19] The band then disappears as the radical cation is further reduced to the neutral species according to reaction (2). When it is further reduced, the bands corresponding to the radical cation, *i.e.*, at about 320 nm and 490 nm, disappear and that at about 370 nm starts to appear beyond store number 20. This arises from the neutral species as shown by controlled potential electrolysis at -1.10 V (*vide infra*).

When the MV^{2+} solution is electrolyzed in the same cell at -1.10 V *vs.* Ag/AgCl electrode, the band at 369 nm was first observed, indicating that the neutral species is generated. As the electrolysis time becomes longer, the band corresponding to the radical cation is seen to increase as a result of reaction (3) and then decay at later times. Shown in Fig-

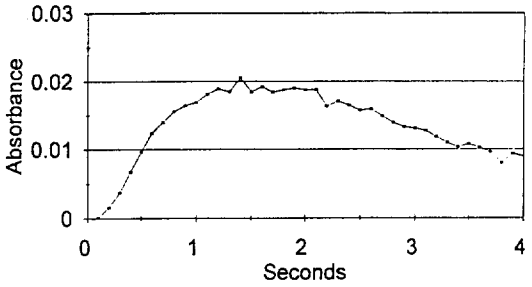

Figure 3. Rise and decay of absorbance values at 490 nm during electrolysis at the Hg pool electrode at −1.10 V in the thin layer cell (TLC).

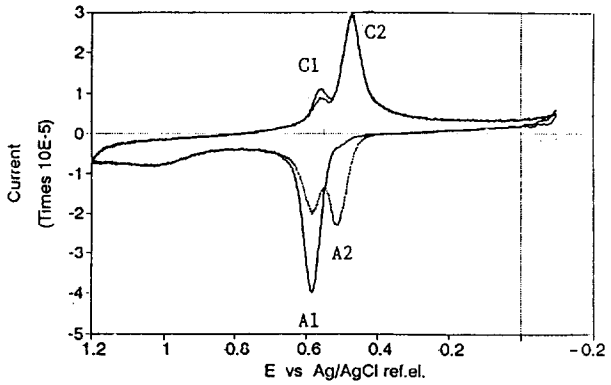

Figure 4. Cyclic voltammogram recorded for 5.1 mM p-aminophenol at Pt in 1.0 *M* H_2SO_4 in the TLC. The scan rate was 2 mV/s.

ure 3 is the rise and decay of the absorption band at 490 nm due to the radical cation. Since the rate of reaction (3) is much faster ($k_f = 6.3 \times 10^7\ M^{-1}$) than the diffusion time scale and thus the radical cation would be produced at a diffusion controlled rate upon the encounter of the neutral species and dication, the rise and decay of the 490 nm band provide an indication of the diffusion of these species toward the reaction zone.

The second redox system studied is the oxidation of p-aminophenol (PAP). PAP is known to form an unstable radical cation upon oxidation, which was detected by the EPR technique in a high flow cell.[20] The electronic transition spectrum of the one electron product, *i.e.*, radical cation, has not been reported due to its short lifetime. Its electrochemistry is described as the generation of short-lived radical cations which undergo a further electron transfer, followed by a chemical reaction to a more stable quinoneimine. The two electron product (quinoneimine) now undergoes a hydrolysis reaction to benzoquinone. The overall reaction may be represented as:

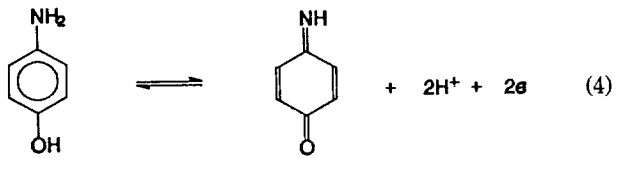

(4)

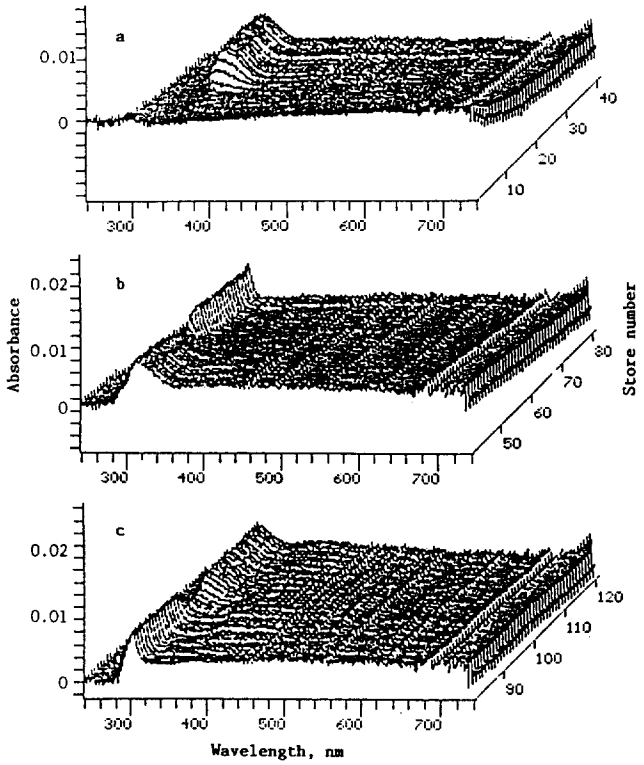

Figure 5. Spectra recorded while the CV shown in Figure 4 is being recorded during the (a) first anodic, (b) first cathodic, and (c) second anodic scans.

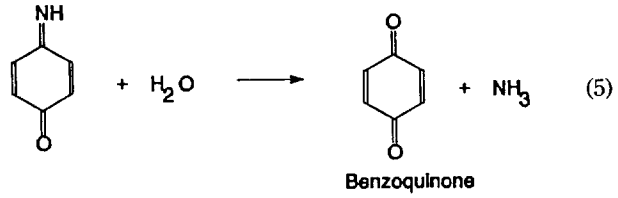

(5)

The cyclic voltammogram (CV) in Figure 4, which was recorded in a thin layer spectroelectrochemical cell at a reflective platinum electrode, shows a sharp anodic peak (A_1) at about 0.60 V and another broad peak at about 1.1 V during the first anodic scan. During the reverse scan, two cathodic peaks C_1 and C_2 are observed. The first cathodic peak, C_1, observed during the reverse scan is attributed to the reduction of the quinoneimine back to PAP. The second cathodic peak, C_2, arises from the reduction of benzoquinone to hydroquinone, which is produced as a result of the following chemical reaction (5). The pseudo first order rate constant of reaction (5) has been reported to be in the range of 0.10-0.13 s^{-1}.[21-23] During the second anodic scan, another anodic peak A_2 is observed for the reoxidation of hydroquinone to benzoquinone along with peak A_1 due to the oxidation of PAP.

A series of spectra recorded during the potential scan are shown in Figure 5. During the forward scan, it is clearly seen that a species absorbing at 312 nm is being generated as the potential increases past the anodic current peak A_1. We assign this absorption band to the quinoneimine produced by reaction (4) because of the fairly high absorption band observed above 370 nm simultaneously with the 312

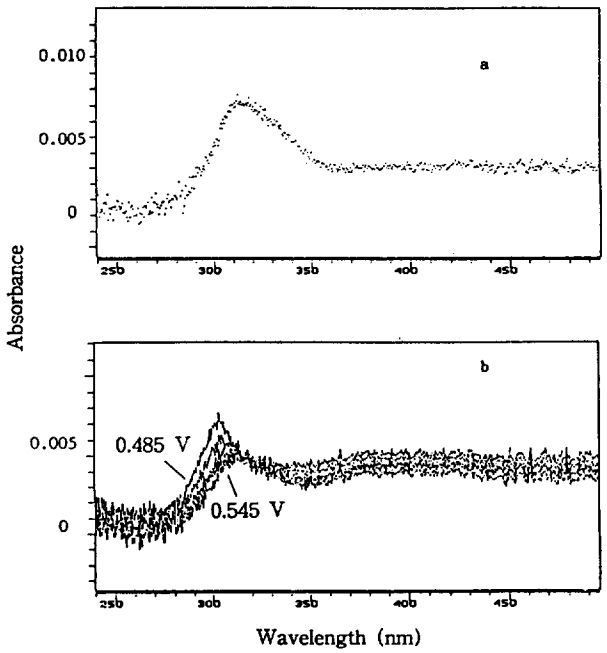

Figure 6. (a) Spectrum recorded at 0.74 V during the forward scan and (b) spectra recorded at 0.545, 0.530, and 0.485 V, respectively, during the reverse scan.

nm band (see Figure 6(b)). Quinoneimine, with its quinoid structure where an electron would be highly conjugated in the excited state, is expected to give a broad absorption band in the longer wavelength region.[24] The quinoneimine can also be regarded as a rigid dication, which has been termed as a bipolaron in oligomeric or polymeric structures. Bipolarons of many organic conducting polymers show broad absorption band in a spectral region of 650-800 nm.[25] The spectra may also contain that of benzoquinone, which is known to have a major absorption band below 300 nm with another very weak absorption band at 405 nm. The latter is not usually observed unless its concentration is significantly high. Although we used faster data acquisition time of as short as 25 ms for recording each spectrum, essentially the same spectra with more noise were observed. Thus, the radical cation must have either a very similar spectral feature to that of quinoneimine or a shorter lifetime than 25 ms. Even for the quinoneimine, the absorbance is so low due to its low molar absorptivity that it may not have been observed by more traditional detectors. We used the integration of 100 per file for the spectra shown here.

The absorption peak of quinoneimine increases rapidly as the potential reaches the anodic CV peak and stays at a more or less steady state throughout the anodic scan (Figure 5). When the potential is reversed, the broad absorption band with its peak at 312 nm decreases gradually as the potential passes through the cathodic CV peak C_1 and is replaced by a sharp absorption band with its maximum at 302 nm (Figure 5(b)), which arises from the absorption by hydroquinone. During the second anodic scan (Figure 5(c)), the hydroquinone band is seen to disappear at the anodic CV peak, A_2, and the quinoneimine band reappears beyond peak A_1. This is a graphic illustration of electrochemical processes taking place during the potential scan.

As the spectra shown here are fairly crowded and it is difficult to see the changes, we singled out a few and showed them in Figure 6. The broad absorption in a longer wavelength region, which is not apparent in spectra shown in Figure 5, is clearly seen Figure 6(a) and (b). The change in the spectral feature for the corresponding electrochemical change is also seen more clearly in Figure 6(b).

Conclusion

We have demonstrated that a spectroelectrochemical system with a spectrograph and CCD detector can monitor spectral changes of many electrochemical reactions in real time during electrochemical experiments. Unfortunately, the systems did not allow very fast measurements to be made due to either relatively low absorbances of the intermediates/products (PAP oxidation) or the too fast reaction rates (methyl viologen reduction). In the case of methyl viologen reduction, the reproportionation reaction (3), is too fast compared to the time scale of the spectral measurements. Although the molar absorptivities of products are sufficiently high, faster acquisition of spectra did not lead to better time-resolved spectra. This is because the reaction is controlled by the diffusion of MV^0 and MV^{2+}; the time for the maximum absorbance shown in Figure 3 indicates merely the maximum amount of MV^+ produced as a result of the largest concentration gradient for MV^0 from the electrode surface and that for MV^{2+} from the solution to the electrode surface.

The setup demonstrates, however, the utility of the technique for monitoring the spectra during an electrochemical reaction in real time. One can follow an electron transfer reaction with reasonably fast following chemical reactions with the present setup. Also, high quantum yields, longer stability, and wider linearity of the detector allow the spectra to be recorded for intermediates or products with low molar absorptivities, with excellent signal-to-noises after extensive averaging. Spectra shown in Figure 5 and 6 demonstrate that this is the case. With extensive averaging, real time spectra with decent signal-to-noise ratios were obtained during the potential scan. In fact, the data acquisition speed for the detector was limited also by the data acquisition software provided by the instrument vendor. The software is far from being optimal and requires a number of improvements in its performance. By obtaining in spectral framing mode, the data acquisition rate can be sped up significantly. Work along this line is currently under way in our laboratory.

Acknowledgement. Grateful acknowledgement is made to Sandia National Laboratories (Contract AE-2151) and Korea Science and Engineering Foundation (Grant 92-25-00-02) for partially supporting this work. S.-i.M. acknowledges her thanks to Ajou University for granting her a sabbatical leave during 1992-93 academic year.

References

1. Kuwana, T.; Darlington, R. K.; Leedy, D. W. *Anal Chem.* **1964**, *36*, 2023.
2. Kuwana, T.; Winograd, N. in *Electroanalytical Chemistry*; Bard, A. J. Ed.; Marcel Dekker: New York, 1974; Vol. 7, p 1.

3. Müller, R. H. ed. *Advances in Electrochemistry and Electrochemical Engineering*; Wiley-Interscience: New York, 1973; Vol. 8.
4. Kuwana, T.; Heineman, W. R. *Acc. Chem. Res.* **1976**, *9*, 241.
5. Miles, R. *SIA, Surf. Interface Anal.* **1983**, **5**, 43.
6. Robinson, J. in *Electrochemistry--Specialist Periodical Reports*; Pletcher, D. Ed.; The Royal Society of Chemistry, Burlington House, London, 1984; Vol. 9.
7. Skully, J. P.; McCreery, R. L. *Anal. Chem.* **1980**, *52*, 1885.
8. (a) Robinson, R. S.; McCreery, R. L. *Anal. Chem.* **1981**, *53*, 997. (b) Robinson, R. S.; McCurdy, C, W.; McCreery, R. L. *ibid.* **1982**, *54*, 2356.
9. Pyun, C.-H.; Park, S.-M. *Anal. Chem.* **1986**, *58*, 251.
10. Zhang, C.; Park, S.-M. *Anal. Chem.* **1988**, *60*, 1639.
11. Zhang, C.; Park, S.-M. *Bull. Korean Chem. Soc.* **1989**, *10*, 302.
12. (a) Kubota, M.; Fujishiro, Y.; Ishida, R. *Spectrochim. Acta*, **1982**, *B37*, 849. (b) Zalewski, E. F.; Duda, C. R. *Appl. Opt.* **1983**, *22*, 2867.
13. Epperson, P. M.; Sweedler, J. V.; Bihorn, R. B.; Sims, G. R.; Denton, M. B. *Anal. Chem.* **1988**, *60*, 282A and 327A.
14. Epperson, P. M.; Denton, M. B. *Anal. Chem.* **1989**, *61*, 1513.
15. Williamson, J. M.; Bowling, R. J.; McCreery, R. L. *Appl. Spectrosc.* **1989**, *43*, 372.
16. Pemberton, J. E.; Sobocinski, R. L.; Sims, G. R. *Appl. Spectrosc.* **1990**, *44*, 328.
17. Allred, C. D.; McCreery, R. L. *Appl. Spectrosc.* **1990**, *44*, 1229.
18. Kosower, E. M.; Cotter, J. L. *J. Am. Chem. Soc.* **1964**, *86*, 5524.
19. Schwartz, W. M. Jr., Ph. D. Dissertation, **1961**, University of Wisconsin, Madison, Wisconsin.
20. Fox, W. M.; Waters, W. A. *J. Chem. Soc.* **1964**, 6010.
21. Testa, A. C.; Reinmuth, W. H. *Anal. Chem.* **1960**, *32*, 1512.
22. Herman, H. B.; Bard, A. J. *Anal. Chem.* **1964**, *36*, 510.
23. Tryk, D. A.; Park, S.-M. *Anal. Chem.* **1979**, *51*, 585.
24. Shim, Y.-B.; Won, M.-S.; Park, S.-M. *J. Electrochem. Soc.* **1990**, *137*, 538.
25. Patil, A. O.; Heeger, A. J.; Wudl, F. *Chem. Rev.* **1988**, *88*, 183.

Photochemical Reactions of Saccharin-α-Silylamine Systems. Desilylmethylation of α-Silylamine *via* Single Electron Transfer Pathway

Ung Chan Yoon*, Young Sim Koh, Hyun Jin Kim, Dong Yoon Jung, Dong Uk Kim, Sung Ju Cho, and Sang Jin Lee

Department of Chemistry, Pusan National University, Pusan 609-735, Korea
Received March 28, 1994

Photochemical reactions of saccharin with tertiary amines were explored. Saccharin was found to undergo an acid-base reaction with N-trimethylsilylmethyl-N,N-diethyl amine to form N-trimethylsilylmethyl-N,N-diethyl ammonium saccharin salt which is in equilibrium with free saccharin and N-trimethylsilylmethyl-N,N-diethyl amine in solution. Photoreaction of N-trimethylsilylmethyl-N,N-diethyl ammonium saccharin in CH_3OH or CH_3CN results in the generation of desilylmethylated product, N,N-diethyl ammonium saccharin mainly along with benzamide. Photoreaction of N-methylsaccharin with N-trimethylsilylmethyl-N,N-diethyl amine in CH_3OH leads to the production of *o*-(N-methylcarbamoyl)-N-ethylbenzenesulfonamide as the major product along with N-methylbenzamide as the minor product. On the other hand, photoreaction of N,N,N-triethyl ammonium saccharin, generated from saccharin and triethylamine, produces N-methylbenzamide as the exclusive product. These photoreactions are quenched by oxygen indicating that triplets of saccharin and N-methylsaccharin are the reactive excited states. Based on the consideration of the redox potentials of saccharin and N-trimethylsilylmethyl-N,N-diethyl amine, and the nature of photoproducts, pathways involving initial triplet state single electron transfer are proposed for photoreactions of the saccharins with the α-silylamine.

Introduction

The photochemistry of imides has been intensively investigated in the past two decades.[1] One subclass in this family, phthalimides, exhibit a variety of photoreactivities including photoreduction, photoaddition, photocyclization, photocycloaddition, and Norrish type I and type II reactions. Studies in the area of single electron transfer (SET) photochemistry using α-silyl electron donors led to the observation that photoinduced sequential SET-desilylation pathways serve as efficient and highly regioselective methods for carbon centered radical generation.[2] Phthalimides are known to undergo smooth photoaddition reactions in methanol or acetonitrile with α-silyl-*n*-electron donors to generate 3-substituted products *via* mechanistic routes which involve sequential SET-desilylation.[3] Similarly phthalimides tethered with α-silyl-n-